Article

Non-Gaussianity of Four-Photon Superpositions of Fock States

Miguel Citeli de Freitas[1] and Viktor V. Dodonov[1,2]* 📙 **0000-0001-7599-209X**

[1]   Institute of Physics, University of Brasilia, P.O. Box 04455, 70919-970 Brasilia, DF, Brazil
[2]   International Center for Physics, University of Brasilia, Brasilia, DF, Brazil
*   Correspondence: vdodonov@unb.br

Abstract: We compare several different measures of non-Gaussianity for two families of four-photon superpositions of the Fock states: even vacuum squeezed states and orthogonal-even coherent states.

---

1. Introduction

Non-Gaussian states play important role in quantum optics. It is enough to remember that the basic Fock states are strongly non-Gaussian. Many families of such states were studied during decades: see, e.g, the review [1]. Recently, a new wave of interest to non-Gaussian states has grown due to possible applications in different areas of the quantum information [2–5]. In this connection, the problem of classifying and quantifying the degree of non-Gaussianity of quantum states attracted the attention of many researchers for the past years [6–40].

It is well known that the following equality holds for any Gaussian state (either pure or mixed):

$$\langle \hat{x}^4 \rangle = 3 \langle \hat{x}^2 \rangle^2. \tag{1}$$

Therefore, one could be tempted to consider as a simple measure of non-Gaussianity the normalized *kurtosis*

$$\mathcal{K} \equiv \langle \hat{x}^4 \rangle / (3 \langle \hat{x}^2 \rangle^2) - 1, \tag{2}$$

which can be easily calculated for many quantum states. However, this parameter has many disadvantages. In particular, it depends on the choice of the representation, as soon as the forms of the wave functions (or density matrices) in the coordinate and momentum representations can be quite different in the most general case.

For this reason, the main trend is to use the statistical operator $\hat{\rho}$ of the system and compare it somehow with the statistical operator $\hat{\rho}_G$ of some reference Gaussian state. Obviously, such measures of non-Gaussianity do not depend on the choice of representation. At this point, one can remember that all non-Gaussian states are "nonclassical". Therefore, it seems natural to look for possible correlations between various measures of "non-Gaussianity" and measures of "non-classicality". The latter ones are frequently based on some kinds of distances between the states under study and certain states (or families of states) selected as reference ones [41–51]. The main and simplest ingredient of these approaches is the trace

$$T \equiv \text{Tr}(\hat{\rho}\hat{\rho}_G) = \langle \psi | \hat{\rho}_G | \psi \rangle, \tag{3}$$

where the second equality holds for any pure state $\hat{\rho} = |\psi\rangle\langle\psi|$. Following this line of reasonings, the authors of paper [6] introduced the measure of *non-Gaussianity* as

$$\delta_T[\hat{\rho}] = \frac{\mathrm{Tr}\left[(\hat{\rho} - \hat{\rho}_G)^2\right]}{2\mathrm{Tr}\left(\hat{\rho}^2\right)} = \frac{\mathrm{Tr}\left(\hat{\rho}^2 + \hat{\rho}_G^2 - 2\hat{\rho}\hat{\rho}_G\right)}{2\mathrm{Tr}\left(\hat{\rho}^2\right)}, \tag{4}$$

where $\hat{\rho}_G$ is the unique Gaussian state with the same first- and second-order moments of quadrature variables as in the state $\hat{\rho}$. For *pure* quantum states with $\mathrm{Tr}\left(\hat{\rho}^2\right) = 1$ the right-hand side of (4) is simplified as

$$\delta_T[|\psi\rangle\langle\psi|] = \frac{1}{2}\left[1 + \mathrm{Tr}\left(\hat{\rho}_G^2\right)\right] - \langle\psi|\hat{\rho}_G|\psi\rangle. \tag{5}$$

Several authors proposed simple measures containing the only positive parameter $\langle\psi|\hat{\rho}_G|\psi\rangle$ in the case of pure quantum states (only this case is considered in the present paper). The measure

$$\delta_F[|\psi\rangle\langle\psi|] = 1 - \sqrt{\langle\psi|\hat{\rho}_G|\psi\rangle} \tag{6}$$

was considered in [16,18,37]. Another measure was proposed in paper [36]:

$$\mathcal{N}_g[|\psi\rangle\langle\psi|] = -\ln\left(\langle\psi|\hat{\rho}_G|\psi\rangle\right). \tag{7}$$

The relative entropy

$$\delta_E[\hat{\rho}] = \mathrm{Tr}[\hat{\rho}\ln(\hat{\rho})] - \mathrm{Tr}[\hat{\rho}_G\ln(\hat{\rho}_G)] \tag{8}$$

was suggested as a measure of non-Gaussianity in [7] (see also [18]). Similar measures were suggested, e.g., in [14] (using the Wehrl entropy in terms of the Husimi Q-function). For pure quantum states we have the formula $\delta_E[\hat{\rho}] = -\mathrm{Tr}[\hat{\rho}_G\ln(\hat{\rho}_G)]$ which does not contain the quantum state $|\psi\rangle$ explicitly.

Our interest to the problem of non-Gaussianity has originated from studies of various generalizations of uncertainty relations. It is well known that all *pure* Gaussian states minimize the Robertson–Schrödinger uncertainty relation [52,53]

$$\mathcal{D} \equiv \sigma_{xx}\sigma_{pp} - \sigma_{xp}^2 - \hbar^2/4 \geq 0. \tag{9}$$

Several generalizations of inequality (9) were aimed on the inclusion of higher-order statistical moments of canonical variables [54–56]. In particular, it can be interesting to know the minimal value of the product $\Pi^{(4)} = \langle\hat{x}^4\rangle\langle\hat{p}^4\rangle$. In view of identity (1), $\Pi^{(4)} \geq 9\hbar^4/16$ for any Gaussian state. However, it was shown in [54] that for specific superpositions of the vacuum and 4th excited Fock states one can achieve the value $\Pi^{(4)} \approx 0,49$. The best known lower limit of $\Pi^{(4)}$ was calculated numerically in Ref. [57] for specific superpositions of the *four-photon* Fock states $|4k\rangle$ with $0 \leq k \leq 6$. Since all states minimizing $\Pi^{(4)}$ are *non-Gaussian*, our initial idea was to try to connect properties of the four-photon superpositions with some measures of non-Gaussianity.

Looking at inequality (9), one can think that the quantity $\mathcal{D}$ itself can be considered as some measure of non-Gaussianity of pure quantum states, as soon as $\mathcal{D} \equiv 0$ for all Gaussian pure states. We may call such measures (including some monotonous functions of $\mathcal{D}$) as $\mathcal{D}$-measures. An example of such an approach is paper [38], where generalizations to the case of mixed quantum states were made on the basis of the so called Wigner-Yanase skew information [58].

Another idea is to replace zero in the right-hand side of (9) with some function containing some measure of non-Gaussianity. This way was taken in papers [15,20], where the following *Gaussianity parameter g* was introduced exactly with this purpose:

$$g = \text{Tr}\,(\hat{\rho}\hat{\rho}_G)\,/\text{Tr}\left(\hat{\rho}_G^2\right). \tag{10}$$

This definition holds for mixed quantum states as well as for pure ones. Obviously, $g = 1$ for any Gaussian state. Unfortunately, there exist non-Gaussian states with $g = 1$ (an example is given in Section 4). This is a disadvantage of the definition (10) (whereas $\delta_T[\hat{\rho}] = 0$ for Gaussian states only). However, it can be useful for detecting the entanglement [29].

Various families of quantum states were analyzed in connection with the non-Gaussianity measures described above. We give a brief and certainly incomplete list of publications, mentioning *pure* quantum states only. Single Fock states were considered in [6,16,21,38]. A table comparing different measures for these states can be found in [38]. Superpositions of two Fock states were studied in [7,8,38]. Various superpositions of two coherent states $|\alpha\rangle$ and $|-\alpha\rangle$ with different weights and phases were considered in papers [6,8,23,25,26,36–38]. Such superpositions include, in particular, the so called even/odd coherent states, introduced in [59] and frequently considered nowadays as simple models of the "Schrödinger cat states"; for numerous generalizations one can consult, e.g., Refs. [60,61]. Various families of photon-added and photon-subtracted states were considered in papers [13,21–23,26,28,34–36,38,62]. Many examples related to all these states were considered in [39].

In this paper, we add two interesting families of pure non-Gaussian states to this list. From all known measures, we choose five examples, when all ingredients can be calculated analytically rather easily: (5)-(8) and (10). In addition, we study the behavior of kurtosis (2), which shows several interesting properties. A similar analysis in the case of cat states was performed in paper [25]. Two selected families are special cases of general four-photon superpositions of the Fock states $\sum_{n=0}^{\infty} c_n |4n\rangle$. There are two motivations for our choice. The first one originated from the observation that almost absolute minimum of the product $\Pi^{(4)}$ can be observed in these states (for an appropriate choice of parameters). The second reason is due to exceptional properties of the four-photon superpositions discussed in Section 2.

The first example, considered in detail in Section 3, is the superposition of two squeezed vacuum states with opposite squeezing parameters [63]:

$$|z\rangle_+ = B\left[\hat{S}(z) + \hat{S}(-z)\right]|0\rangle, \qquad \hat{S}(z) \equiv \exp\left[\frac{1}{2}\left(z\hat{a}^{\dagger 2} - z^*\hat{a}^2\right)\right]. \tag{11}$$

Using the well known methods of the $su(1,1)$ algebra (see, e.g., [64,65]), the exponential in the definition of the squeezing operator $\hat{S}(z)$ can be disentangled as

$$\hat{S}(z) = \hat{U}(z)\exp\left[-\frac{1}{2}\ln[\cosh(|z|)]\left(\hat{a}\hat{a}^{\dagger} + \hat{a}^{\dagger}\hat{a}\right)\right]\hat{U}^{\dagger}(-z), \tag{12}$$

where

$$\hat{U}(z) = \exp\left[\frac{z\tanh(|z|)}{2|z|}\hat{a}^{\dagger 2}\right].$$

Consequently,

$$\hat{S}(z)|0\rangle = [\cosh(|z|)]^{-1/2}\sum_{n=0}^{\infty}\frac{\sqrt{(2n)!}}{2^n(n)!}\left[\frac{z}{|z|}\tanh(|z|)\right]^n|2n\rangle, \tag{13}$$

so that we have the following expansion of the state (11) over the Fock basis for $z = re^{i\theta}$ with $r \geq 0$:

$$|z\rangle_+ = \mathcal{N} \sum_{n=0}^{\infty} \frac{\sqrt{(4n)!}}{2^{2n}(2n)!} [e^{i\theta} \tanh(r)]^{2n} |4n\rangle. \tag{14}$$

Similar superpositions with $\theta = 0$ were considered recently in [32]. More general superpositions of squeezed states were studied in [63,66,67], but we confine ourselves here to the states (11). We shall call them *even vacuum squeezed states* (EVSS).

The second family of states, considered in Section 4, consists of superpositions of four coherent states with equal amplitudes, but with phases shifted by $\pi/2$:

$$|\psi\rangle_{4\alpha} = B \sum_{k=0}^{3} |\alpha \exp(ik\pi/2)\rangle = \mathcal{N} \sum_{n=0}^{\infty} \frac{\alpha^{4n}}{\sqrt{(4n)!}} |4n\rangle, \tag{15}$$

$$B^2 = \frac{\exp\left(|\alpha|^2\right)}{16 E_4\left(|\alpha|^2\right)}, \quad \mathcal{N}^2 = \frac{1}{E_4\left(|\alpha|^2\right)}, \quad E_4(x) \equiv \sum_{n=0}^{\infty} \frac{x^{4n}}{(4n)!} = \frac{1}{2} \left[\cosh(x) + \cos(x)\right]. \tag{16}$$

Such kinds of states were studied for a long time from different points of view. They were named "four-photon states" [68], "orthogonal-even coherent states" [69], "pair cat states" [70], "compass states" [71], "four-headed cat states" [72]. Recently, such states were considered in studies [32,73,74]. Following [69], we use the abbreviation OECS for the state (15).

2. Non-gaussianity of arbitrary four-photon superpositions and mixtures

The four-photon superpositions $\sum_{n=0}^{\infty} c_n |4n\rangle$ possess several specific properties, which permit us to simplify many calculations. The first nice feature is the existence of the following simple relations between the lowest order statistical moments:

$$\langle \hat{x} \rangle = \langle \hat{p} \rangle = \langle \hat{x}\hat{p} + \hat{p}\hat{x} \rangle = 0, \quad \langle \hat{x}^2 \rangle = \langle \hat{p}^2 \rangle, \quad \langle \hat{x}^4 \rangle = \langle \hat{p}^4 \rangle. \tag{17}$$

They are consequences of the relations between the quadratures and annihilation/creation operators,

$$\hat{x} = \left(\hat{a} + \hat{a}^\dagger\right)/\sqrt{2}, \quad \hat{p} = \left(\hat{a} - \hat{a}^\dagger\right)/(i\sqrt{2}),$$

(hereafter we use dimensionless variables with $\hbar = 1$). Hence, the Gaussian reference state for *any* four-photon superposition is described by means of the *thermal* statistical operator, which depends on the only parameter $\langle \hat{x}^2 \rangle$. In particular, the corresponding Gaussian Wigner function and coordinate probability density have the following forms:

$$W_G(q,p) = \langle \hat{x}^2 \rangle^{-1} \exp\left[-\frac{q^2 + p^2}{2\langle \hat{x}^2 \rangle}\right], \quad \rho_G(q,q) = (2\pi\langle \hat{x}^2 \rangle)^{-1/2} \exp\left(-\frac{q^2}{2\langle \hat{x}^2 \rangle}\right), \tag{18}$$

Respectively,

$$\text{Tr}\left(\hat{\rho}_G^2\right) = \sigma^{-1}, \quad \sigma \equiv 2\langle \hat{x}^2 \rangle. \tag{19}$$

The normalized thermal statistical operator of the harmonic oscillator can be written also in terms of the annihilation/creation operators as

$$\hat{\rho}_G = \left(1 - e^{-\beta}\right) \exp\left(-\beta \hat{a}^\dagger \hat{a}\right), \tag{20}$$

where the "inverse temperature" parameter β can be expressed in terms of parameter σ as follows,

$$e^{-\beta} = \frac{\sigma - 1}{\sigma + 1}. \tag{21}$$

Consequently, the operator $\hat{\rho}_G$ is diagonal in the Fock basis:

$$\hat{\rho}_G = \frac{2}{\sigma + 1} \sum_{n=0}^{\infty} \left(\frac{\sigma - 1}{\sigma + 1} \right)^n |n\rangle\langle n|. \tag{22}$$

The relative entropy measure of non-Gaussianity for *pure* quantum states can be written as follows,

$$\delta_E[\hat{\rho}] = \frac{\beta}{e^{\beta} - 1} - \ln\left(1 - e^{-\beta}\right) = \frac{\sigma + 1}{2}\ln(\sigma + 1) - \frac{\sigma - 1}{2}\ln(\sigma - 1) - \ln 2. \tag{23}$$

Now, let us consider an arbitrary operator $\hat{\rho} = \sum_{m,n} \rho_{mn}|m\rangle\langle n|$ and and arbitrary *diagonal* operator (in the Fock basis) $\hat{\rho}_d = \sum_n p_n|n\rangle\langle n|$. The trace of their product contains only diagonal elements ρ_{nn}:

$$\mathrm{Tr}\,(\hat{\rho}\hat{\rho}_d) \equiv T = \sum_n \rho_{nn} p_n. \tag{24}$$

Formula (24) tells us that the measures (5), (6), (7) and (10) do not depend on the phases θ and ϕ of the complex numbers z and α characterizing the states $|z\rangle_+$ (11) and $|\psi\rangle_{4\alpha}$ (15). The concrete dependences on $|z|$ and $|\alpha|$ of the cited measures are considered in the following sections. For pure quantum states considered in this paper, other non-Gaussianity measures can be written in terms of T and σ as follows:

$$\delta_T = \frac{1 + \sigma}{2\sigma} - T, \quad \delta_F = \sqrt{1 - T}, \quad \mathcal{N}_g = -\ln(T), \quad g = \sigma T. \tag{25}$$

3. Non-Gaussianity measures in EVSS

In view of formula (13), the wave function of the squeezed state in the coordinate representation $\psi_z(x) \equiv \langle x|\hat{S}(z)|0\rangle$ can be written as a series over the Hermite polynomials:

$$\psi_z(x) = \frac{\exp\left(-x^2/2\right)}{\left[\sqrt{\pi}\cosh(|z|)\right]^{1/2}} \sum_{n=0}^{\infty} \left(\frac{z\tanh(|z|)}{4|z|} \right)^n \frac{H_{2n}(x)}{n!}. \tag{26}$$

Using formula 5.12.1.4 from [75],

$$\sum_{k=0}^{\infty} \frac{t^k}{k!} H_{2k}(x) = (1 + 4t)^{-1/2} \exp\left(\frac{4tx^2}{1 + 4t} \right), \tag{27}$$

one can obtain the following expression:

$$\psi_z(x) = \pi^{-1/4} [u_+(z)]^{-1/2} \exp\left[-\frac{u_-(z)}{2u_+(z)} x^2 \right], \tag{28}$$

where

$$u_{\pm}(z) = \cosh(|z|) \pm \frac{z}{|z|}\sinh(|z|) = u_{\mp}(-z). \tag{29}$$

Consequently, the wave function $\Psi_z(x)$ of EVSS (11) in the coordinate representation has the form

$$\Psi_z(x) = N \left\{ u_+^{-1/2} \exp\left[-\frac{u_- x^2}{2u_+} \right] + u_-^{-1/2} \exp\left[-\frac{u_+ x^2}{2u_-} \right] \right\}, \tag{30}$$

where N is the normalization factor. The following relations are useful for calculations:

$$u_+ u_-^* = 1 + i\kappa, \quad \kappa = \sinh(2r)\sin(\theta), \tag{31}$$

$$|u_\pm|^2 = \cosh(2|z|) \pm \sinh(2|z|)\cos(\theta), \tag{32}$$

$$|u_+|^2 |u_-|^2 = 1 + \kappa^2, \quad |u_+|^2 + |u_-|^2 = 2\cosh(2|z|). \tag{33}$$

The probability density has the form

$$|\Psi_z(x)|^2 = |N|^2 \left\{ \frac{1}{|u_+|} \exp\left(-\frac{x^2}{|u_+|^2} \right) + \frac{1}{|u_-|} \exp\left(-\frac{x^2}{|u_-|^2} \right) \right.$$
$$\left. + 2\mathrm{Re}\left[(u_+ u_-^*)^{-1/2} \exp\left(-\frac{x^2 \cosh(2|z|)}{u_+ u_-^*} \right) \right] \right\}. \tag{34}$$

After the integration, using identities (31)-(33), we arrive at the remarkable result that the normalization constant depends on the only parameter $c \equiv \sqrt{\cosh(2|z|)}$:

$$|N|^2 = \frac{B}{2\sqrt{\pi}}, \quad B = \frac{c}{1+c}. \tag{35}$$

Calculating the Fourier transform of function $\psi_z(x)$, one obtains the wave function of the squeezed state in the momentum representation,

$$\tilde{\psi}_z(p) = \pi^{-1/4} [u_-(z)]^{-1/2} \exp\left[-\frac{u_+(z)}{2u_-(z)} p^2 \right]. \tag{36}$$

Consequently, $\tilde{\Psi}_z(p)$ is given by the same formula (30), with x replaced by p. Therefore, all statistical moments of the coordinate and momentum coincide in the EVSS.

Simple calculations show that the second-order moment also depends on the only parameter c:

$$\langle \hat{x}^2 \rangle = \frac{c^5 + 1}{2c^2 (1+c)} \equiv \sigma/2. \tag{37}$$

Note that $\sigma \approx c^2$ when $c \gg 1$. If $r \ll 1$, then, $c \approx 1 + r^2 - r^4/6$ and $\sigma \approx 1 + 3r^4$.

The fourth-order moment depends on r and θ:

$$\langle \hat{x}^4 \rangle (r,\theta) = \frac{3B}{4} \left\{ \cosh^2(2r) + \cos^2(\theta)\sinh^2(2r) + \frac{1 - \sin^2(\theta)\sinh^2(2r)}{[\cosh(2r)]^{5/2}} \right\}. \tag{38}$$

The minimum of $\langle \hat{x}^4 \rangle (r,\theta)$ for the fixed value of r is achieved for $\theta = \theta_* = \pm\pi/2$, so that

$$\langle \hat{x}^4 \rangle (r,\theta_*) = \frac{3B}{4} \left\{ \cosh^2(2r) + \frac{1 - \sinh^2(2r)}{[\cosh(2r)]^{5/2}} \right\}. \tag{39}$$

Numerical calculations yield $\langle \hat{x}^4 \rangle_{min} = 0.6987$ and $\Pi^{(4)}_{min} = 0.4882$ for $r = r_* = 0.2690$ and $c_* = 1.072$. This value is very close to the minimal value $\Pi^{(4)}_{min} = 0.4878$ found in study [57]. In our case, $\langle \hat{x}^2 \rangle (r_*, \theta_*) = 0.5072$, only a slightly higher value than in the vacuum state. Note that $\Pi^{(4)}(z_*) = 7.3743 \left[\Pi^{(2)}(z_*) \right]^2$. If the state were Gaussian, then the coefficient in the right-hand side would be equal to 9.

For small values of r we have $\langle \hat{x}^4 \rangle (r, \theta) \approx (3/4) \left[1 + 2r^2 \cos(2\theta) \right]$. Figure 1 shows the probability density (34) for different values of the squeezing parameter r and phase θ. We see that the probability density looks close to the Gaussian for $r < 0.5$, whereas it becomes obviously non-Gaussian for higher values of r. Pay attention to the inverse order of lines in the left-hand and right-hand sides of Figure 1. These parts look totally different for big values of r. Therefore, it is interesting to understand how the non-Gaussianity measures correlate with these visual observations.
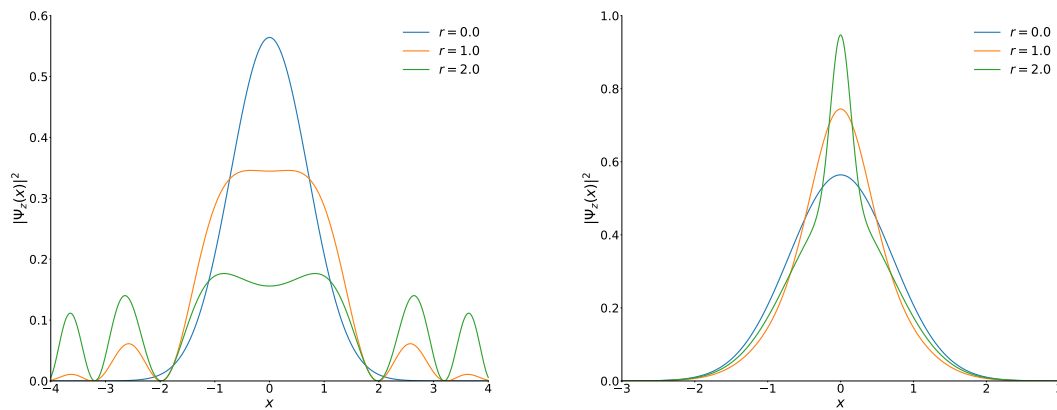

Figure 1. The probability density (34) of EVSS for different values of the squeezing parameter r. Left: $\theta = \pi/2$. Right: $\theta = 0$.

The Wigner function of state (30) equals

$$W_z(q, p) = B \Big\{ \exp \left[-p^2 |u_+|^2 - q^2 |u_-|^2 + 2\kappa pq \right] + \exp \left[-p^2 |u_-|^2 - q^2 |u_+|^2 - 2\kappa pq \right]$$
$$+ 2[\cosh(2r)]^{-1/2} \mathrm{Re} \Big(\exp \left[2ipq \tanh(2r) \cos(\theta) - p^2 \frac{1 - i\kappa}{\cosh(2r)} - q^2 \frac{1 + i\kappa}{\cosh(2r)} \right] \Big) \Big\}. \tag{40}$$

This function is invariant with respect to the rotation by 90 degrees in the phase plane: $q \to p$, $p \to -q$. Note that $W_z(0, 0) = 2$ for any value of parameter z, as it must be for any symmetrical pure state [76]. One can verify the following expansion of formula (40) for small values of q and p:

$$W_z(q, p) \approx 2 \left[1 - 2\langle \hat{x}^2 \rangle \left(q^2 + p^2 \right) \right]. \tag{41}$$

Remember that we use dimensionless variables, assuming formally $\hbar = 1$. The expansion (41) indicates that function W_z is strongly non-Gaussian, unless the squeezing parameter r is close to zero. Indeed, a similar expansion of function (18) has the form

$$W_G(q, p) \approx \langle \hat{x}^2 \rangle^{-1} \left[1 - \frac{q^2 + p^2}{2\langle \hat{x}^2 \rangle} \right].$$

Therefore, the non-Gaussianity of W_z is clearly demonstrated by the narrow peak nearby the origin of the width proportional to $\langle \hat{x}^2 \rangle^{-1/2}$: see Figure 2. Note that the section $W_z(q,0)$ of the total Wigner function
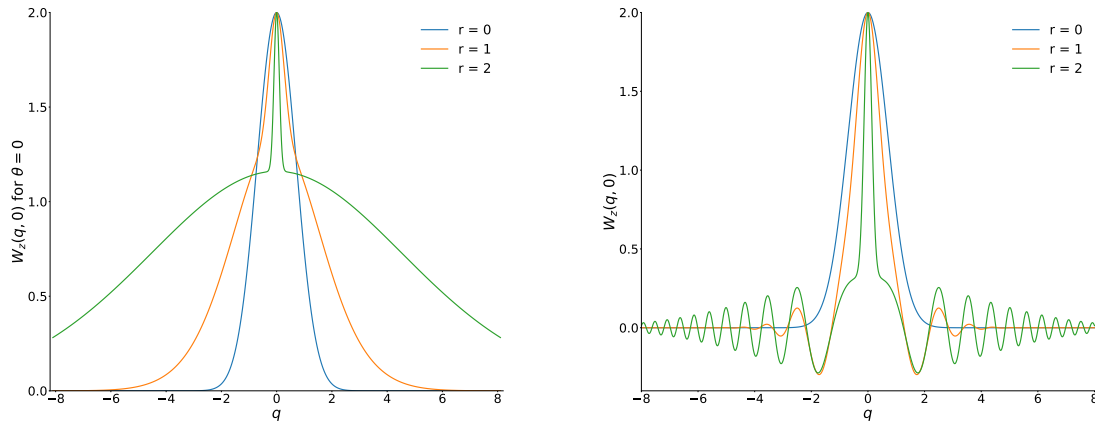

Figure 2. The section $W_z(q,0)$ of EVSS for different values of the squeezing parameter r and phase θ. Left: $\theta = 0$; $r = 0, 1.0, 2.0$. Right: $\theta = \pi/2$, the same values of r.

with $\theta = 0$ is positive in the whole interval $-\infty < q < \infty$. However, $W_z(q,0)$ with $\theta = \pi/2$ shows strong oscillations and negative values if r is not too small, in accordance with the Hudson theorem [77]. Plots of the "diagonal" section $W_z(q,q)$ are similar to those for $W_z(q,0)$, although with an "inversion" of the left and right plots with respect to the phase θ.

The sum (24) with coefficients ρ_{nn} following from formula (13) seems too complicated. In this case, a simpler way to calculate the trace $\text{Tr}(\hat{\rho}\hat{\rho}_G)$ is to use the formula $\text{Tr}(\hat{\rho}\hat{\rho}_G) = \int W W_G dq dp / (2\pi)$, which contains only Gaussian integrals. Using identities (31)-(33) we obtain the formula

$$\text{Tr}(\hat{\rho}_z \hat{\rho}_G) \equiv T = \frac{2c}{1+c} \left\{ \left[\sigma^2 + 2c^2\sigma + 1 \right]^{-1/2} + \left[\left(\sigma^2 + 1 \right) c^2 + 2\sigma \right]^{-1/2} \right\}, \tag{42}$$

where $\sigma = \sigma(c)$ was defined in Equation (37). As was explained in Section 2, this trace does not contain the phase θ. If $\sigma \approx c^2 \gg 1$, then $T \approx 2/(\sigma\sqrt{3})$.

Plots of measures (23) and (25) as functions of parameter c are given in Figure 3. They are compared with the plots of the normalized kurtosis $\mathcal{K}$ (2). Three coefficients $\delta[\rho_z](c)$ grow monotonously from 0 at $c = 1$ to their asymptotic values as $c \to \infty$, and nothing exceptional is noticed for $c = c_*$. The coefficient $g(c)$ grows initially, attains a wide maximum $g_{max} \approx 1.27$ at $r_{max} \approx 1.33$ (or $c_{max} \approx 2.68$), and decays monotonously to $g_\infty = 2/\sqrt{3} \approx 1.155$ as $c \to \infty$. However, the maximum of $g(c)$ apparently has no correlation with the minimum of $\langle \hat{x}^4 \rangle$. For $r \ll 1$ we obtain $g \approx 1 + 9r^4/8$ and $\delta_T[\rho_z] \approx 3r^4/8$.

The behavior of the normalized kurtosis is more interesting. For $\theta = \pi/2$, $\mathcal{K}$ is negative for small values of the squeezing parameter r, attaining the minimal value $\mathcal{K}_{min} = -0.1111$ at $r_{min} = 0.3504$. However, $\mathcal{K}$ becomes positive for $r > 0.549$, and it goes to zero as c^{-1} when $c \to \infty$. On the other hand, $\mathcal{K}$ is always positive for $\theta \leq \pi/4$. Its asymptotic behavior for $c \to \infty$ is given by the formulas $\mathcal{K} \approx 1 + 2/c$ for $\theta = 0$ and $\mathcal{K} \approx 1/2 + 3/(2c)$ for $\theta = \pi/4$. In all the cases, $\mathcal{K}$ has maximums: $\mathcal{K}_{max} \approx 0.3757$ at $r = 1.1011$ if $\theta = \pi/2$, $\mathcal{K}_{max} \approx 1.0592$ at $r = 1.0911$ if $\theta = \pi/4$ and $\mathcal{K}_{max} \approx 1.7427$ at $r = 1.0911$ if $\theta = 0$. However, we do not see any correlation of these maximums with the behavior of the Wigner functions or the functions $g(c)$ and $\delta[\rho_z](c)$.
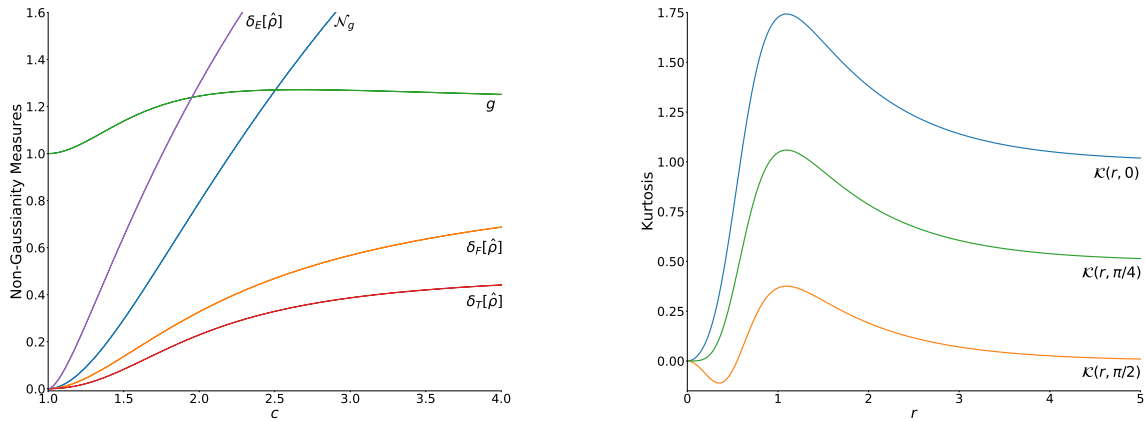
Figure 3. The behavior of the non-Gaussianity measures (left) and kurtosis (right) as functions of parameters c and r, respectively, for the Even Vacuum Squeezed States.

4. Non-Gaussianity measures in OECS

In the case of OECS (15), the second-order mean value of the coordinate and momentum does not depend on the phase of complex parameter α [56]):

$$\langle \hat{x}^2 \rangle = \langle \hat{p}^2 \rangle \equiv \sigma/2 = \frac{1}{2} + a\frac{\sinh(a) - \sin(a)}{\cosh(a) + \cos(a)}, \quad \alpha \equiv \sqrt{a}e^{i\phi}. \tag{43}$$

On the other hand,

$$\langle \hat{x}^4 \rangle = \langle \hat{p}^4 \rangle = \frac{3}{4} + \frac{a^2}{2}\cos(4\phi) + 3\frac{a[\sinh(a) - \sin(a)] + a^2[\cosh(a) - \cos(a)]/2}{\cosh(a) + \cos(a)}. \tag{44}$$

The minimum $\langle \hat{x}^4 \rangle_{min} = 0.6999$ is achieved for $\cos(4\phi) = -1$ at $a_* = 0.4489$.

The normalized wave function of OECS in the coordinate representation has the following form:

$$\psi_{4\alpha}(x) = \frac{\exp\left(-x^2/2\right)}{2\pi^{1/4}\sqrt{E_4\left(|\alpha|^2\right)}} \left[\cosh(\sqrt{2}\alpha x)\exp\left(-\alpha^2/2\right) + \cos(\sqrt{2}\alpha x)\exp\left(\alpha^2/2\right)\right]. \tag{45}$$

Remember that $\alpha = |\alpha|e^{i\phi}$ is a complex number. Therefore, the behavior of the wave function strongly depends on the phase ϕ if $|\alpha| \gg 1$. For example, if α is real and $|\alpha x| \ll 1$, then,

$$\psi_{4\alpha}(x) \approx \frac{\cosh\left(a/2\right)}{\pi^{1/4}\sqrt{E_4\left(a\right)}} \left\{1 - \frac{x^2}{2}\left[1 + 2a\tanh\left(a/2\right)\right]\right\}, \quad a = |\alpha|^2.$$

In this case, the hight of the maximum $\psi_{4\alpha}(0)$ practically does not depend on α, but its width is strongly reduced, compared with the case of $\alpha = 0$. On the other hand, for $\phi = \pi/4$ we have

$$\psi_{4\alpha}(x) = \frac{\sqrt{2}\exp\left(-x^2/2\right)\left[\cosh(|\alpha|x)\cos(|\alpha|x)\cos(|\alpha|^2/2) + \sinh(|\alpha|x)\sin(|\alpha|x)\sin(|\alpha|^2/2)\right]}{\pi^{1/4}\sqrt{\cosh(|\alpha|^2) + \cos(|\alpha|^2)}}. \tag{46}$$

This function turns into zero at $x = 0$ if $|\alpha|^2 = \pi$. Plots of functions (45) and (46) are shown in Figure 4 for different (not very big) values of $|\alpha|$. Figure 5 shows the coordinate probability density for bigger values of parameter $a = |\alpha|^2$. A significant difference between the cases of phases $\phi = 0$ and $\phi = \pi/4$ is clearly seen.
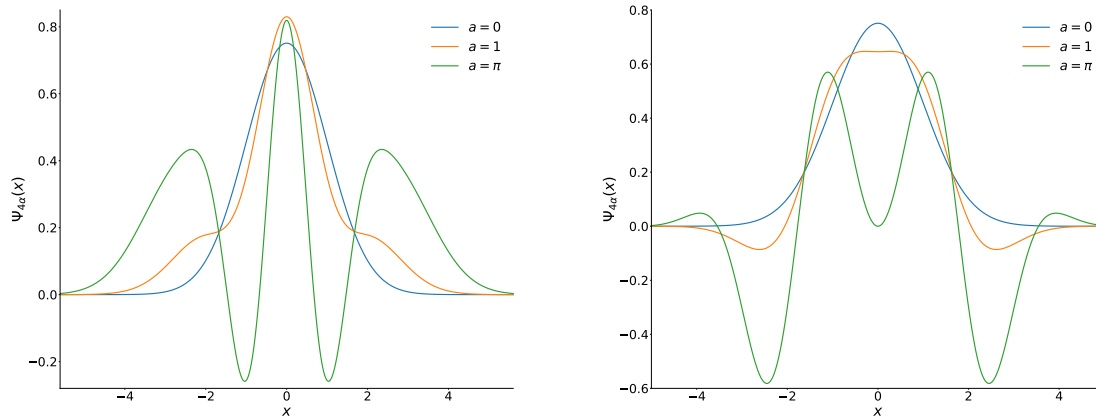

Figure 4. Real wave functions of OECS for different values of parameter $\alpha = \sqrt{a}\exp(i\phi)$. Left: $\phi = 0$. Right: $\phi = \pi/4$.
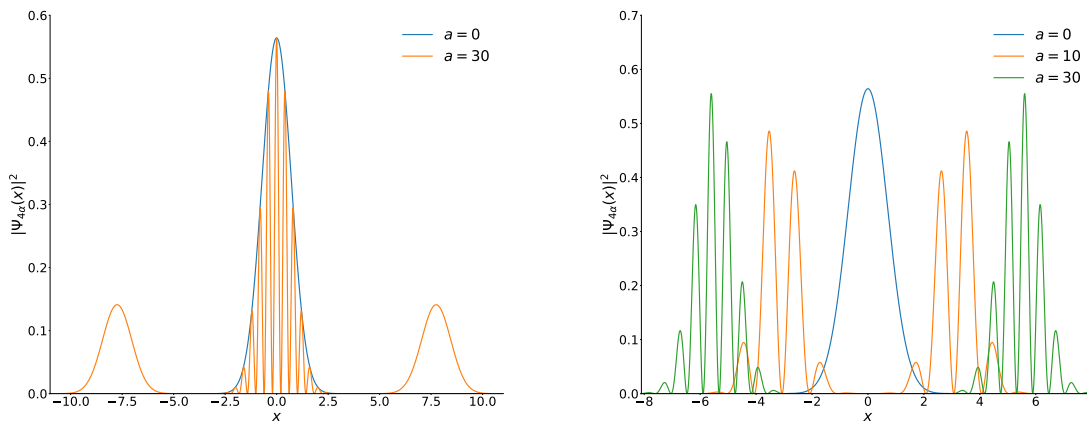

Figure 5. The coordinate probability density of OECS for different values of parameter $a = |\alpha|^2$ and phase ϕ. Left: $\phi = 0$. Right: $\phi = \pi/4$.

The Wigner function is the sum of 16 exponential terms with $\alpha_k = \alpha i^k$ and $\alpha_j = \alpha i^j$,

$$W_{4\alpha}(q, p) = \frac{\exp\left(-q^2 - p^2\right)}{8E_4\left(|\alpha|^2\right)} \sum_{k,j=0}^{3} \exp\left[\sqrt{2}q\left(\alpha_k + \alpha_j^*\right) - i\sqrt{2}p\left(\alpha_k - \alpha_j^*\right) - \alpha_k\alpha_j^*\right]. \tag{47}$$

If α is a real number, then,

$$
\begin{aligned}
W_{4\alpha}(q,p) \;=\; & \frac{\exp\left(-q^2 - p^2\right)}{4E_4\left(|\alpha|^2\right)} \left\{ e^{-\alpha^2}\left[\cosh(2\gamma q) + \cosh(2\gamma p)\right] + e^{\alpha^2}\left[\cos(2\gamma q) + \cos(2\gamma p)\right] \right. \\
& + 2\cos(\alpha^2)\left(\cos[\gamma(q+p)]\cosh[\gamma(q+p)] + \cos[\gamma(q-p)]\cosh[\gamma(q-p)]\right) \\
& \left. + 2\sin(\alpha^2)\left(\sin[\gamma(q+p)]\sinh[\gamma(q+p)] + \sin[\gamma(q-p)]\sinh[\gamma(q-p)]\right) \right\},
\end{aligned}
\tag{48}
$$

where $\gamma = \alpha\sqrt{2}$. Plots of the sections $W_{4\alpha}(q,0)$ and $W_{4\alpha}(q,q)$ of function (48) are given in Figure 6 for $\alpha^2 = 0, \pi/2, \pi$. Although the section $W_{4\alpha}(q,0)$ is positive in the whole interval $-\infty < q < \infty$, the section
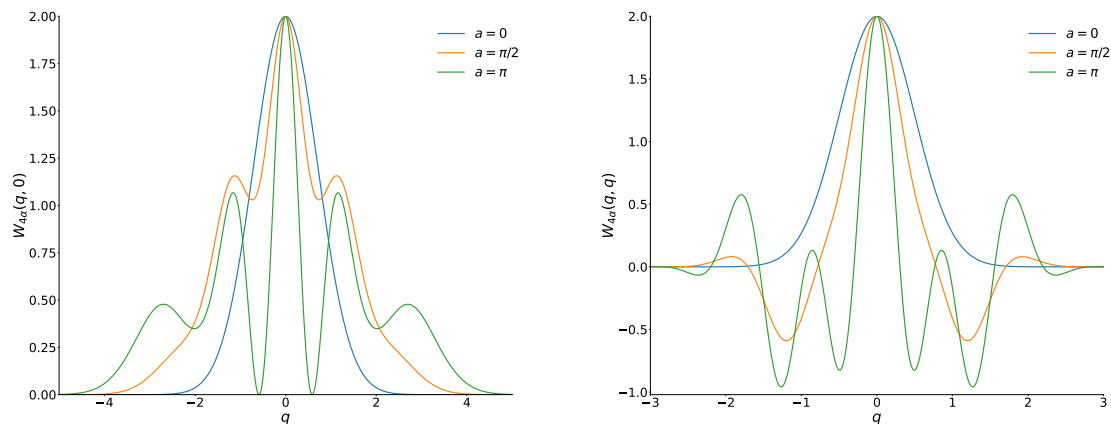

Figure 6. The sections of function $W_{4\alpha}(q,p)$ for different values of real parameter $\alpha = \sqrt{a}$. Left: $W_{4\alpha}(q,0)$. Right: $W_{4\alpha}(q,q)$.

$W_{4\alpha}(q,q)$ shows strong oscillations and negative values. In all the cases, the width of the central peak diminishes with the increase of parameter a.

If $\alpha = |\alpha|\exp(i\pi/4)$, then,

$$
\begin{aligned}
W_{4\alpha}(q,p) \;=\; & \frac{\exp\left(-q^2 - p^2\right)}{2E_4\left(|\alpha|^2\right)} \left\{ e^{-|\alpha|^2}\cosh(2|\alpha|q)\cosh(2|\alpha|p) + e^{|\alpha|^2}\cos(2|\alpha|q)\cos(2|\alpha|p) \right. \\
& + \cos(|\alpha|^2)\left[\cos(2|\alpha|p)\cosh(2|\alpha|p) + \cos(2|\alpha|q)\cosh(2|\alpha|q)\right] \\
& \left. + \sin(|\alpha|^2)\left[\sin(2|\alpha|p)\sinh(2|\alpha|p) + \sin(2|\alpha|q)\sinh(2|\alpha|q)\right] \right\}.
\end{aligned}
\tag{49}
$$

Plots of sections $W_{4\alpha}(q,0)$ and $W_{4\alpha}(q,q)$ of function (49) are given in Figure 7 for $|\alpha| = 0$ and $|\alpha| = 3$.

In the case involved, the trace $\text{Tr}(\hat{\rho}\hat{\rho}_G)$ can be easily calculated by means of formula (24), because it is reduced to the simple series $E_4(x)$ defined in Equation (16):

$$
\text{Tr}(\hat{\rho}\hat{\rho}_G) \equiv T = \frac{2E_4(ae^{-\beta})}{(\sigma+1)E_4(a)}, \qquad e^{-\beta} = \frac{\sigma-1}{\sigma+1}.
\tag{50}
$$

Plots of measures (23) and (25) as functions of parameter a are given in Figure 8, together with the plots of kurtosis. We see that the behavior of functions $g(a)$ and $\mathcal{K}(a)$ is quite different from the behavior of functions $g(c)$ and $\mathcal{K}(c)$ in the case of EVSS, shown in Fig. 3. Function $g(a)$ is especially interesting. Indeed, function $E_4(x)$ behaves as $e^x/4$ for $x \gg 1$. If $a \gg 1$, then $\sigma \approx 1 + 2a$. In this limit case, we
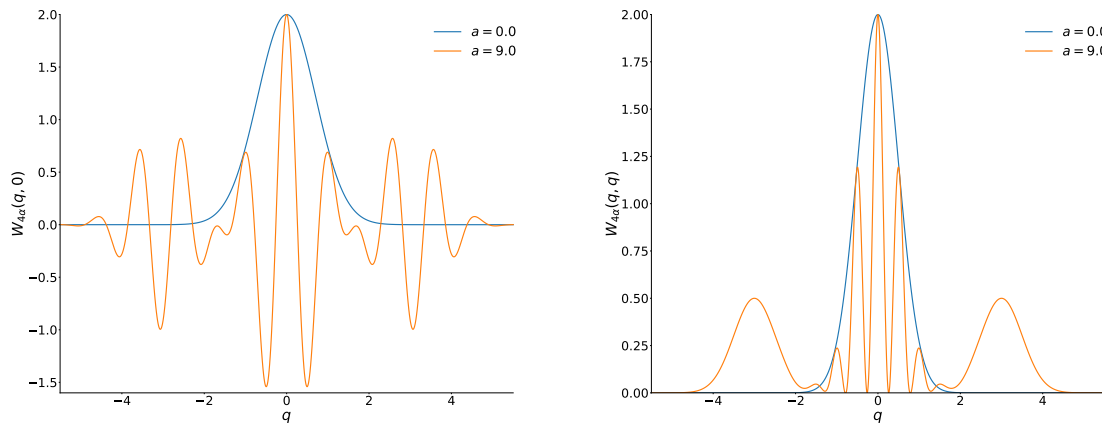
Figure 7. The sections of function $W_{4\alpha}(q, p)$ for $\alpha = |\alpha| \exp(i\pi/4)$. Left: $W_{4\alpha}(q, 0)$. Right: $W_{4\alpha}(q, q)$.

have $e^{-\beta} \approx a/(1 + a) \approx 1 - 1/a$. Neglecting the term $1/a$, one could think that $E_4\left(ae^{-\beta}\right) \approx E_4(a)$ for $a \to \infty$, arriving at the asymptotic value $g(\infty) = 2$. However, a more correct calculation yields the ratio $E_4(ae^{-\beta})/E_4(a) \approx E_4(a-1)/E_4(a) \approx 1/e$ for $a \gg 1$. Therefore, the correct asymptotic value is $g(\infty) = 2/e \approx 0.74$, in full accordance with Figure 8. Hence, $T \approx 2/(e\sigma)$ when $a \gg 1$ and $\sigma \approx 1 + 2a \gg 1$. The maximum value $g_{max} \approx 1.1735$ is attained at $a = 1.4615$. In addition, $g(a) < 1$ for $a > 2.209$.
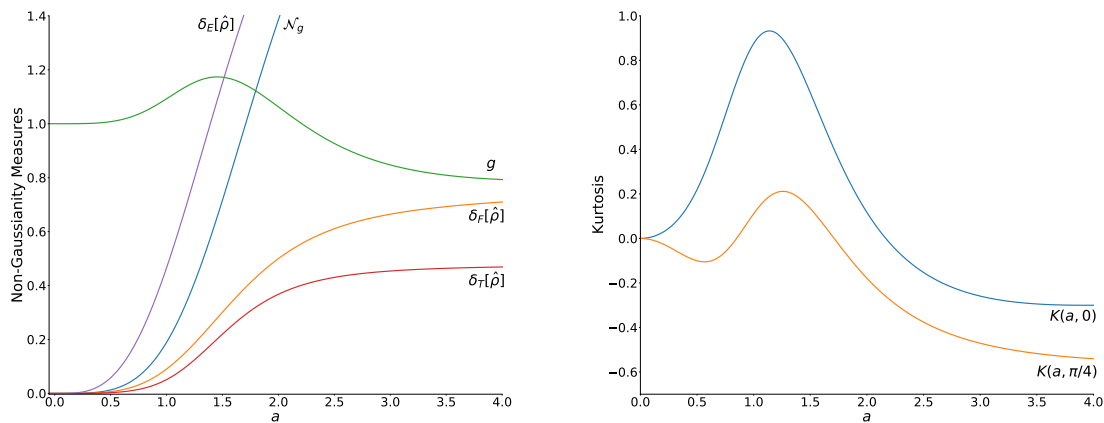

Figure 8. The behavior of the non-Gaussianity measures (left) and kurtosis (right) as functions of parameter a for the Orthogonal Even Coherent States.

The evolution of the kurtosis depends on the phase ϕ. If $\phi = \pi/4$, the local minimum $\mathcal{K}_{min} = -0.1052$ is achieved at $a = 0.5658$ and maximum $\mathcal{K}_{max} = 0.2115$ at $a = 1.2577$. In addition, $\mathcal{K} = 0$ at $a = 0.8490$ and $a = 1.7103$. If $\phi = 0$, one can see the maximum $\mathcal{K}_{max} = 0.9323$ at $a = 1.1391$. When $a \to \infty$, the kurtosis tends to the asymptotic value $\mathcal{K}(\infty) = [\cos(4\phi) - 3]/6$. The minimal possible asymptotic value $-2/3$ corresponds to $\phi = \pi/4$. This is an example of distribution possessing the property $\langle \hat{x}^4 \rangle \approx \langle \hat{x}^2 \rangle^2$. This equality is explained by the right-hand side of Figure 5: when $a \to \infty$, the distribution (strongly non-Gaussian) is concentrated symmetrically in two small regions. On the other hand, if $\phi = 0$, then the distribution remains concentrated nearby the origin, with two symmetric relatively small remote wings:

see the left-hand part of Figure 5. As a consequence, the ratio $\langle \hat{x}^4 \rangle / \langle \hat{x}^2 \rangle^2$ turns out twice bigger than for $\phi = \pi/4$.

5. Comparison of non-Gaussianity of EVSS and OECS

It is interesting to compare the degrees of non-Gaussianity of two families of states: EVSS and OECS. For this purpose, these degrees must be calculated for equal values of some parameter. A relevant physical parameter could be the state energy, or, equivalently for the four-photon superpositions, the coordinate variance $\sigma/2$. However, the dependences $\sigma(r)$ (for EVSS) and $\sigma(a)$ (for OECS) are rather complicated, so that the inverse functions $r(\sigma)$ and $a(\sigma)$ can be found only numerically. For this reason, we choose the simple common parameter in the form of the inverse fidelity between each component of the superpositions and the vacuum state: $\tau = |\langle 0|\alpha \rangle|^{-2}$ and $\tau = |\langle 0|z \rangle|^{-2}$. Then,

$$a = \ln(\tau), \qquad \cosh(r) = \tau, \quad c = \sqrt{2\tau^2 - 1}. \tag{51}$$

Figure 9 shows the measures $\delta_T[\hat{\rho}](\tau)$ and $g(\tau)$ for EVSS and OECS. According to this figure, the EVSS are
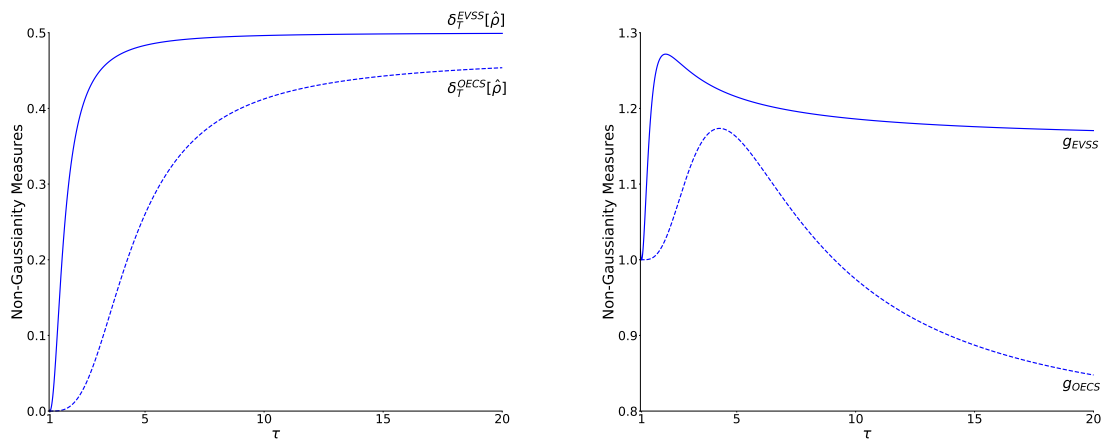

Figure 9. Non-Gaussianity measures as functions of the inverse fidelity τ between the vacuum state and components of two kinds of superpositions.

"more non-Gaussian" than OECS for all values of parameter τ, especially for small values of this parameter. However, it is difficult to confirm this evaluation looking at plots of the probability distributions and Wigner functions. Probably, attempts to quantify different families of states according to their "non-Gaussianity" have no real sense.

6. Conclusions

We have compared five different measures of non-Gaussianity for two interesting four-photon superpositions of the Fock states. Four measures show a monotonous growth when parameters characterizing the "size" of superpositions are increased. However, it is difficult to choose any of these measures as the "best" one: all of them seem more or less equivalent, at least for *pure* quantum states studied in this paper. The behavior of the "Gaussianity" measure (10) is quite different. It is non-monotonous (apparently due to the presence of the factor $\text{Tr}\left(\hat{\rho}_G^2\right)$ in the denominator), so this measure hardly can be used to compare the degree of Gaussianity of different states. Moreover, all the measures do not take into account a "fine structure" of quantum states. In particular, all of them do not distinguish between the

states with different phases but equal absolute values of complex parameters z or α, while the plots of the probability densities and Wigner functions show the importance of these phases. In this connection, the behavior of kurtosis (which strongly depends on the phases) can provide an important additional information. It is interesting that "large" even superpositions of coherent states (with $a \gg 1$) show the "sub-Gaussian" behavior. Moreover, selecting the specific phase of parameter α one can obtain the ratio $\langle \hat{x}^4 \rangle / (\langle \hat{x}^2 \rangle)^2$ as close to unity as desired. On the contrary, almost all even superpositions of the vacuum squeezed states are "super-Gaussian", except for small values of complex parameter z with properly chosen phases.

Author Contributions: M.C.F.: analytical and numerical calculations, plotting figures; V.V.D.: conceptualization, methodology, analytical calculations and writing the paper. All authors have read and agreed to the published version of the manuscript.

Conflicts of Interest: The authors declare no conflict of interest.

References

1. Dodonov, V.V. 'Nonclassical' states in quantum optics: a 'squeezed' review of the first 75 years. *J. Opt. B: Quantum Semiclass. Opt.* **2002**, *4*, R1–R33.
2. Dell'Anno, F.; De Siena, S.; Adesso, G.; Illuminati, F. Teleportation of squeezing: optimization using non-Gaussian resources. *Phys. Rev. A* **2010**, *82*, 062329.
3. Zhuang, Q.; Shor, P.W.; Shapiro, J.H. Resource theory of non-Gaussian operations. *Phys. Rev. A* **2018**, *97*, 052317.
4. Takagi, R.; Zhuang, Q. Convex resource theory of non-Gaussianity. *Phys. Rev. A* **2018**, *97*, 062337.
5. Albarelli, F.; Genoni, M.G.; Paris, M.G.A.; Ferraro, A. Resource theory of quantum non-Gaussianity and Wigner negativity. *Phys. Rev. A* **2018**, *98*, 052350.
6. Genoni, M.G.; Paris, M.G.A.; Banaszek, K. Measure of the non-Gaussian character of a quantum state. *Phys. Rev. A* **2007**, *76*, 042327.
7. Genoni, M.G.; Paris, M.G.A.; Banaszek, K. Quantifying the non-Gaussian character of a quantum state by quantum relative entropy. *Phys. Rev. A* **2008**, *78*, 060303.
8. Genoni, M.G.; Paris, M.G.A. Quantifying non-Gaussianity for quantum information. *Phys. Rev. A* **2010**, *82*, 052341.
9. Barbieri, M.; Spagnolo, N.; Genoni, M.G.; Ferreyrol, F.; Blandino, R.; Paris, M.G.A.; Grangier, P.; Tualle-Brouri, R. Non-Gaussianity of quantum states: An experimental test on single-photon-added coherent states. *Phys. Rev. A* **2010**, *82*, 063833.
10. Mandilara, A.; Karpov, E.; Cerf, N.J. Gaussianity bounds for quantum mixed states with a positive Wigner function. *J. Phys.: Conf. Ser.* **2010**, *254*, 012011.
11. Filip, R.; Mišta Jr., L. Detecting quantum states with a positive Wigner function beyond mixtures of Gaussian states. *Phys. Rev. Lett.* **2011**, *106*, 200401.
12. Ježek, M.; Straka, I.; Mičuda, M.; Dušek, M.; Fiurášek, J.; Filip, R. Experimental Test of the Quantum Non-Gaussian Character of a Heralded Single-Photon State. *Phys. Rev. Lett.* **2011**, *107*, 213602.
13. Xu, X.X.; Yuan, H.C.; Hu, L.-Y.; Fan, H.-Y. Non-Gaussianity of photon-added-then-subtracted squeezed vacuum state. *Optik* **2012**, *123*, 16–20.
14. Ivan, J.S.; Kumar, M.S.; Simon, R. A measure of non-Gaussianity for quantum states. *Quantum Inf. Process* **2012**, *11*, 853–872.
15. Mandilara, A.; Cerf, N.J. Quantum uncertainty relation saturated by the eigenstates of the harmonic oscillator. *Phys. Rev. A* **2012**, *86*, 030102.

16. Ghiu, I.; Marian, P.; Marian, T.A. Measures of non-Gaussianity for one-mode field states. *Phys. Scr.* **2013**, *T153*, 014028.

17. Genoni, M.G.; Palma, M.L.; Tufarelli, T.; Olivares, S.; Kim, M.S.; Paris, M.G.A. Detecting quantum non-Gaussianity via the Wigner function. *Phys. Rev. A* **2013**, *87*, 062104.

18. Marian, P.; Marian, T.A. Relative entropy is an exact measure of non-Gaussianity. *Phys. Rev. A* **2013**, *88*, 012322.

19. Lachman, L.; Filip, R. Robustness of quantum nonclassicality and non-Gaussianity of single-photon states in attenuating channels. *Phys. Rev. A* **2013**, *88*, 063841.

20. Mandilara, A.; Karpov, E.; Cerf, N.J. Purity- and Gaussianity-bounded uncertainty relations *J. Phys. A: Math. Theor.* **2014**, *47*, 045302.

21. Hughes, C.; Genoni, M.G.; Tufarelli, T.; Paris, M.G.A.; Kim, M.S. Quantum non-Gaussianity witnesses in phase space. *Phys. Rev. A* **2014**, *90*, 013810.

22. Xu, X.-X.; Luo, W.-W.; Zhang, H.-L.; Ma, S.-J. Nonclassical and non-Gaussian properties of states generated by the superposed photon added-and-subtracted operation on squeezed vacuum. *Optik* **2014**, *125*, 4190–4195.

23. Seshadreesan, K.P.; Dowling, J.P.; Agarwal, G.S. Non-Gaussian entangled states and quantum teleportation of Schrödinger-cat states. *Phys. Scr.* **2015**, *90*, 074029.

24. Park, J.; Zhang, J.; Lee, J.; Ji, S.-W.; Um, M.; Lv, D.; Kim, K.; Nha, H. Testing nonclassicality and non-Gaussianity in phase space. *Phys. Rev. Lett.* **2015**, *114*, 190402.

25. Xiang, S.-H.; Song, K.-H. Quantum non-Gaussianity of single-mode Schrödinger cat states based on kurtosis. *Eur. Phys. J. D* **2015**, *69*, 260.

26. Son, W. Role of quantum non-Gaussian distance in entropic uncertainty relations *Phys. Rev. A* **2015**, *92*, 012114.

27. Park, J.; Nha, H. Demonstrating nonclassicality and non-Gaussianity of single-mode fields: Bell-type tests using generalized phase-space distributions. *Phys. Rev. A* **2015**, *92*, 062134.

28. Xiao, J.; Xiong, C.; Yuan, H.-C.; Chen, L.; Zhu, X.-F. Non-positive Wigner function and non-Gaussianty generated by multiple creation-then-annihilation coherent state. *Int. J. Theor. Phys.* **2016**, *55*, 1719–1727.

29. Hertz, A.; Karpov, E.; Mandilara, A.; Cerf, N.J. Detection of non-Gaussian entangled states with an improved continuous-variable separability criterion. *Phys. Rev. A* **2016**, *93*, 032330.

30. Park, J.; Lu, Y.; Lee, J.; Shen, Y.; Zhang, K.; Zhang, S.; Zubairy, M.S.; Kim, K.; Nha, H. Revealing nonclassicality beyond Gaussian states via a single marginal distribution. *Proc. Nat. Ac. Sci.* **2017**, *114*, 891–896.

31. Park, J.; Lee, J.; Ji, S.-W.; Nha, H. Quantifying non-Gaussianity of quantum-state correlation. *Phys. Rev. A* **2017**, *96*, 052324.

32. Happ, L.; Efremov, M.A.; Nha, H.; Schleich, W.P. Sufficient condition for a quantum state to be genuinely quantum non-Gaussian. *New J. Phys.* **2018**, *20*, 023046.

33. Xiang, S.-H.; Wen, W.; Zhao, Y.-J.; Song, K.-H. Evaluation of the non-Gaussianity of two-mode entangled states over a bosonic memory channel via cumulant theory and quadrature detection. *Phys. Rev. A* **2018**, *97*, 042303.

34. Kühn, B.; Vogel, W. Quantum non-Gaussianity and quantification of nonclassicality. *Phys. Rev. A* **2018**, *97*, 053823.

35. Berrada, K.; Eleuch, H. Measure of non-Gaussianity for photon-added nonlinear coherent states. *Int. J. Geom. Meth. Mod. Phys.* **2018**, *15*, 1850158.

36. Baek K.; Nha, H. Non-Gaussianity and entropy-bounded uncertainty relations: Application to detection of non-Gaussian entangled states. *Phys. Rev. A* **2018**, *98*, 042314.

37. Xiang, S.-H.; Zhao, Y.-J.; Xiang, C.; Wen, W.; Long, X.-W. A method for efficiently estimating non-Gaussianity of continuous-variable quantum states. *Eur. Phys. J. D* **2020**, *74*, 16.

38. Fu, S.; Luo, S.; Zhang, Y. Quantifying non-Gaussianity of bosonic fields via an uncertainty relation. *Phys. Rev. A* **2020**, *101*, 012125.

39. Zhang, Y.; Luo, S. Quantifying non-Gaussianity via the Hellinger distance. *Theor. Math. Phys.* **2020**, *204*, 1046–1058.

40. Hloušek, J.; Ježek, M.; Fiurášek, J. Direct experimental certification of quantum non-Gaussian character and Wigner function negativity of single-photon detectors. *Phys. Rev. Lett.* **2021**, *126*, 043601.

41. Hillery, M. Nonclassical distance in quantum optics. *Phys. Rev. A* **1987**, *35*, 725–732.

42. Dodonov, V.V.; Man'ko, O.V.; Man'ko, V.I.; Wünsche, A. Energy-sensitive and "classical-like" distances between quantum states *Phys. Scr.* **1999**, *59*, 81–89.

43. Dodonov, V.V.; Man'ko, O.V.; Man'ko, V.I.; Wünsche, A. Hilbert–Schmidt distance and nonclassicality of states in quantum optics. *J. Mod. Opt.* **2000**, *47*, 633–654.

44. Zyczkowski K.; Slomczynski W. The Monge metric on the sphere and geometry of quantum states. *J. Phys. A: Math. Gen.* **2001**, *34*, 6689–6722.

45. Malbouisson, J.M.C.; Baseia B. On the measure of nonclassicality of field states. *Phys. Scr.* **2003**, *67*, 93–98.

46. Dodonov, V.V.; Renó, M.B. Classicality and anticlassicality measures of pure and mixed quantum states. *Phys. Lett. A* **2003**, *308*, 249–255.

47. Marian, P.; Marian, T.A.; Scutaru, H. Distinguishability and nonclassicality of one-mode Gaussian states. *Phys. Rev. A* **2004**, *69*, 022104.

48. Klimov, A.B.; Sánchez-Soto, L.L.; Yustas, E.C.; Söderholm, J.; Björk, G. Distance-based degrees of polarization for a quantum field. *Phys. Rev. A* **2005**, *72*, 033813.

49. Rivas, A.; Luis, A. Intrinsic metrological resolution as a distance measure and nonclassical light. *Phys. Rev. A* **2008**, *77*, 063813.

50. Miranowicz, A.; Bartkiewicz, K.; Pathak, A.; Peřina Jr., J.; Chen, Y.-N.; Nori, F. Statistical mixtures of states can be more quantum than their superpositions: Comparison of nonclassicality measures for single-qubit states. *Phys. Rev. A* **2015**, *91*, 042309.

51. Marian, P.; Marian, T.A. A geometric measure of non-classicality. *Phys. Scr.* **2020**, *95*, 054005.

52. Schrödinger, E. Zum Heisenbergschen Unschärfeprinzip. *Sitzungsberichte der Preussischen Akademie der Wissenschaften. Physikalisch-mathematische Klasse*, Berlin, Germany, 1930; pp. 296–303.

53. Robertson, H.P. A general formulation of the uncertainty principle and its classical interpretation. Phys. Rev. **1930**, *35*, 667.

54. Dodonov, V.V.; Man'ko, V.I. Generalization of the uncertainty relations in quantum mechanics. In: *Invariants and the Evolution of Nonstationary Quantum Systems* (Proceedings of Lebedev Physics Institute, Vol. 183); Markov, M.A., Ed.; Nova Science: Commack, New York, USA, 1989; pp. 3–101.

55. Ivan, J.S.; Mukunda, N.; Simon, R. Moments of non-Gaussian Wigner distributions and a generalized uncertainty principle: I. The single-mode case. *J. Phys. A: Math. Gen.* **2012**, *45*, 195305.

56. Citeli, M.F.; Dantas, V. M.; Dodonov, V.V. Minimal products of coordinate and momentum uncertainties of high orders: significant and weak high-order squeezing. *Entropy* **2020**, *22*, 980.

57. Lynch, R.; Mavromatis, H.A. *N*th (even)-order minimum uncertainty products. *J. Math. Phys.* **1990**, *31*, 1947–1951.

58. Wigner, E.P.; Yanase, M.M. Information contents of distributions. *Proc. Nat. Acad. Sci. USA* **1963**, *49*, 910–918.

59. Dodonov, V.V.; Malkin, I.A.; Man'ko, V.I. Even and odd coherent states and excitations of a singular oscillator. *Physica* **1974**, *72*, 597–615.

60. Bužek, V.; Knight, P.L. Quantum interference, superposition states of light, and nonclassical effects. In: *Progress in Optics, vol. XXXIV*, Wolf, E., Ed.; North Holland: Amsterdam, The Netherlands, 1995; pp. 1–158.

61. Man'ko, V.I. Even and odd coherent states and tomographic representation of quantum mechanics and quantum optics. In: *Theory of Nonclassical States of Light*, Dodonov, V.V.; Man'ko, V.I., Eds.; Taylor & Francis: London, Great Britain, 2003; pp. 219–240.

62. Tang, X.-B.; Gao, F.; Wang, Y.-X.; Wu, J.-G.; Shuang, F. Non-Gaussian features from excited squeezed vacuum state. *Opt. Commun.* **2015**, *345*, 86–98.

63. Sanders, B.C. Superposition of two squeezed vacuum states and interference effects. *Phys. Rev. A* **1989**, *39*, 4284–4287.

64. R.R.Puri, *Mathematical Methods of Quantum Optics*; Springer: Berlin, Germany, 2001

65. Wünsche, A. Squeezed states. In: *Theory of Nonclassical States of Light*, Dodonov, V.V.; Man'ko, V.I., Eds.; Taylor & Francis: London, Great Britain, 2003; pp. 95-152.

66. Xin, Z.Z.; Wang, D.B.; Hirayama, M.; Matumoto, K. Even and odd two-photon coherent states of the radiation field. *Phys. Rev. A* **1994**, *50*, 2865–2869.

67. Barbosa, Y.A.; Marques, G.C.; Baseia, B. Generalized superposition of two squeezed states: generation and statistical properties. *Physica A* **2000**, *280*, 346–361.

68. Hach III, E.E.; Gerry, C.C. Four photon coherent states. Properties and generation. *J. Mod. Opt.* **1992**, *39*, 2501–2517.

69. Lynch, R. Simultaneous fourth-order squeezing of both quadrature components. *Phys. Rev. A* **1994**, *49*, 2800–2805.

70. Souza Silva, A.L.; Mizrahi, S.S.; Dodonov, V.V. Effect of phase-sensitive reservoir on the decoherence of pair-cat coherent states. *J. Russ. Laser Res.* **2001**, *22*, 534–544.

71. Zurek, W.H. Sub-Planck structure in phase space and its relevance for quantum decoherence. *Nature* **2001**, *412*, 712–717.

72. Lee, S.-Y.; Lee, C.-W.; Nha, H.; Kaszlikowski, D. Quantum phase estimation using a multi-headed cat state. *J. Opt. Soc. Am. B* **2015**, *32*, 1186–1192.

73. Mirrahimi, M.; Leghtas, Z.; Albert, V.V.; Touzard, S.; Schoelkopf, R.J.; Jiang, L.; Devoret, M.H. Dynamically protected cat-qubits: a new paradigm for universal quantum computation. *New J. Phys.* **2014**, *16*, 045014.

74. Akhtar, N.; Sanders, B.C.; Navarrete-Benlloch, C. Sub-Planck structures: Analogies between the Heisenberg-Weyl and SU(2) groups. *Phys. Rev. A* **2021**, *103*, 053711.

75. Prudnikov, A.P.; Brychkov, Yu.A.; Marichev, O.I. *Integrals and Series. Volume 2. Special Functions*; Taylor & Francis: London, UK, 2002.

76. Dodonov, V.V. Wigner functions and statistical moments of quantum states with definite parity. *Phys. Lett. A* **2007**, *364*, 368–371.

77. Hudson, R.L. When is the Wigner quasi-probability density non-negative? *Rep. Math. Phys.* **1974**, *6*, 249–252.